THEORETICAL AND EXPERIMENTAL INVESTIGATION OF THE BUCKLING AND POST BUCKLING CHARACTERISTICS OF FLAT CARBON FIBRE REINFORCED PLASTIC (CFRP) PANELS SUBJECTED TO COMPRESSION OR SHEAR LOADS

P. Vestergren and L. Knutsson

The Aeronautical Research Institute
of Sweden (FFA)
Stockholm

Abstract

A number of tests were carried out on different CFRP structural elements. These consisted of flat, unstiffened and stiffened panels loaded in compression and flat and U-shaped beams loaded in shear. The main purpose of the investigation was to determine the buckling and post-buckling characteristics and their dependance on the lay-up configuration. The buckling behaviour was studied by the shadow Moire method.

In addition, a theoretical investigation of the buckling behaviour was made using the STAGSC code. In all tests with unstiffened panels the ultimate load well exceeded the buckling load, whereas the compression loaded stiffened panels collapsed at a load only slightly higher than the buckling load. The theoretical and experimental results showed reasonably good agreement.

I. Introduction

The strength of composite materials has been investigated rather thoroughly, both experimentally and theoretically. The stability properties of composite structures, however, are still rather unknown and the purpose of a series of tests, carried out at the FFA, was to give information of the buckling and post buckling behaviour of different composite structures.

The level of ambition of this investigation was to perform static tests on three types of CFRP panels subjected to pure compression or shear loads, and to evaluate to what extent the buckling loads safely may be exceeded before any material damage would occur in the panels. The effects of different lay-up configurations on the buckling behavior of the specimens were also studied to some extent as well as permanent deformation of the specimens when unloaded from specific load levels. In addition to the tests, theoretical analyses were performed - mainly by use of the finite difference method - for comparison with the experimentally obtained values of buckling and fracture loads.

The investigation was sponsored by The Defence Materiel Administration (FMV) and Saab-Scania Aerospace division. Saab-Scania also provided the shear test panels, while the panels subjected to compression were manufactured at the FFA.

In the future further tests have been planned for the evaluation of the buckling characteristics of CFRP panels. Especially stiffened panels will be evaluated in this investigation.

II. Experimental analysis

TEST SPECIMENS

Specimens subjected to compression loads

Two types of panels were manufactured and tested at the FFA. One flat plate with three hat stiffeners bonded to the plate was made from carbon fibre epoxi prepreg Rigidite 5208/T300. Both stiffeners and panel plate had the lay-up configuration, $[0_2 / \pm 45]_{S8}$. The geometrical configuration of the panel is shown in Fig. 1.

Also two flat unstiffened panels were manufactured from the same material as the stiffened panel. The panels were layered in the following order, $[(\pm 60)_2 / 0_2]_{S12}$ and $[0_2 / (\pm 60)_2]_{S12}$. The length and width of these panels were 320 x 370 mm.

The laminates of both types of panels were autoclave cured with the vacuum-bag technique. The hat stiffeners were formed in a mold and were cured separately.

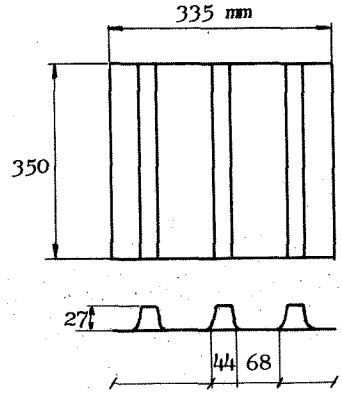

Figure 1. Geometrical configuration of the stiffened panel

Specimens subjected to shear loads

The shear loaded test specimens consisted of three flat and three U-shaped beams. The geometry and lay-up configuration is shown in Fig. 2. The material used in all specimens was carbon fibre epoxi prepreg Thornell 300/Rigidite 5208 and the fibre content was 65 %.

Panel No.	Lay-up configuration
1	$[(\pm 45)_4]_S$
2	$[90/(\pm 45)_4]_S$
3	$[90_2/\pm 45]_S$

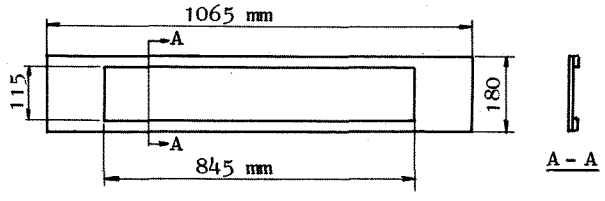

U-beam No.	Lay-up configuration WEB	FLANGE
1	$[90/(\mp 45)_3]_S$	$[(\pm 45)_{3F}/90/(\mp 45)_3]_S$
2	- " -	$[(0/90)_F/(\pm 45)_{2F}/90/(\mp 45)_3]_S$
3	- " -	$[(0/90)_{3F}/90/(\mp 45)_3]_S$

F denotes fabric.

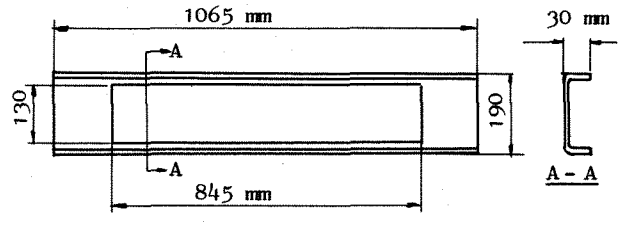

Figure 2. Geometry and lay-up configuration of plane and U-shaped shear panels

In order to investigate the influence of the fibre orientation on the buckling load, three different lay-up configurations were used in the flat panels. Special interest has been paid to, how the percentage 90^o layers (i.e. fibre direction perpendicular to the load direction) affected the ratio P_u/P_c, where P_u is the ultimate load and P_c is the buckling load. At the tests with the U-shaped beams, the main purpose was to investigate how different stiffnesses of the flanges affected the buckling load. Hence, the lay-up configuration of the web was the same in all three U-beams, whereas the flanges had different orientation of the fibres. See Fig. 2. The torsional stiffnesses for the flanges of U-beams 1, 2 and 3 were $K \cdot 32400$ Nmm^2, $K \cdot 27100$ Nmm^2 and $K \cdot 16610$ Nmm^2 respectively. K is a constant.

TEST PROCEDURE

Compression

The loaded ends of the stiffened panel were potted in Araldite D into two steel forms to prevent local failure there as the panel was tested in axial compression. This measure provided approximately clamped edge conditions, whereas the vertical ends were only restricted from movements in the lateral direction (simply supported). In order to evaluate buckling loads and load distribution in the panel, strain gages were bonded to the surfaces of the panel and to the crowns of the stiffeners. The shadow Moire´method was used to study the lateral deflections of the unstiffened panel surface. Fig. 3 illustrates the principle of the shadow Moire´method.

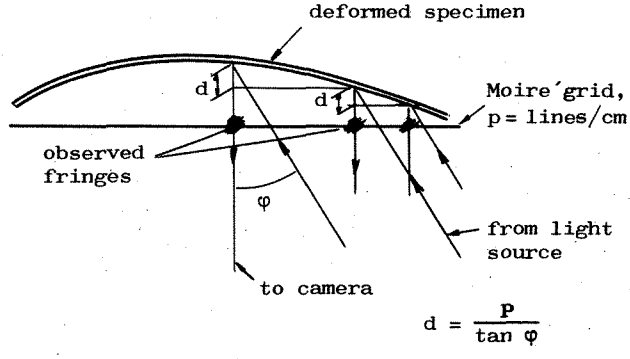

Figure 3. Principle of the shadow Moire´ method. The observed fringes are contours of constant depth (d)

The Moire´ fringes pattern was recorded by a video equipment during loading conditions, so that the buckling behaviour of the panel could be studied after the tests.

The loaded ends of the unstiffened panels were placed into cut-open ball bearings to provide approximately simply supported edge conditions. The vertical ends were held in position by rigid steel rulers, like the vertical ends of the stiffened panel. Evaluation of buckling loads and post-buckling behaviour was made by the shadow Moire´ method.

Load was applied stepwise and the panels were unloaded from each load level to evaluate the appearance of permanent deformation. From the load levels where permanent deformation was observed, load was applied continuously until the panels collapsed.

Shear

The shear testing device used at FFA consists of a floor mounted frame with two horizontal beams, the lower of which is horizontally movable. The test specimens are mounted between two covering plates which are bolted to the horizontal beams of the test jigg.

The load is then applied to the test specimens by moving the lower horizontal beam by use of a hydraulic jack.

With this method, the boundary conditions of the test specimens are close to simple support. The shear deformations of the panels and U-beams were measured by use of dial gauges and the lateral deflection was studied with the shadow Moire' method. In addition the strains were measured by use of rosette strain gauges. The load was applied to the test specimens in steps and after certain load steps the panels were unloaded and the permanent deformations were measured.

During the tests, the Moire' pattern was filmed with a TV camera and occurring sounds of material failure were recorded with a tape-recorder.

RESULTS

Compression

The compression loaded panels were not perfectly flat. Especially the stiffened panel became slightly curved when the stiffeners were bonded to the panel plate, which affected the load distribution in the various parts of the panel. Thus, at low loads before any local buckling occurred in the panel, the panel plate was more strained than the crowns of the stiffeners. Local buckling in the plate appeared at approximately 10 kN and the panel collapsed at 13 kN, resulting in fibre buckling and delamination of layers in all sections of the panel. Fig. 4 illustrates the buckling characteristics of the stiffened panel at 12.5 kN The Moire' fringe pattern also indicates the effects of the initial imperfection in the panel, which obviously reduced the stability of the panel.

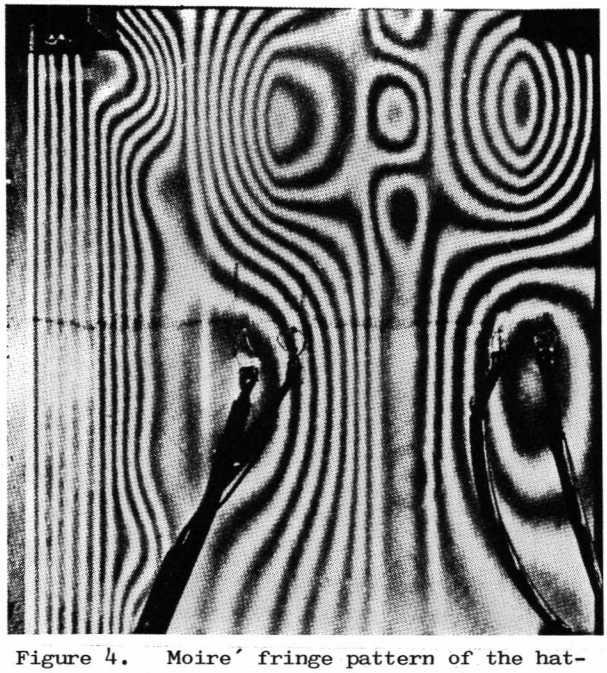

Figure 4. Moire' fringe pattern of the hat-stiffened, compression loaded panel at 12.5 kN

The unstiffened panels had small initial imperfections which triggered the global buckling in half wave mode immediately at load application. As seen in Fig. 5, lateral deflection at centre of panels was accelerated from approximately 200 N for both panels, indicating the buckling loads. At higher loads the centre of panel 2 - having 0^{o}-layers at the panel surfaces - was more deflected than panel 1, which was largerly deflected near loaded ends due to less bending stiffness for bending around horizontal axis. The Moire' patterns of the panels photographed from TV monitor immediately prior to the collapse loads are shown in Fig. 6. Panel 1 collapsed at 30 kN and panel 2 at 35 kN.

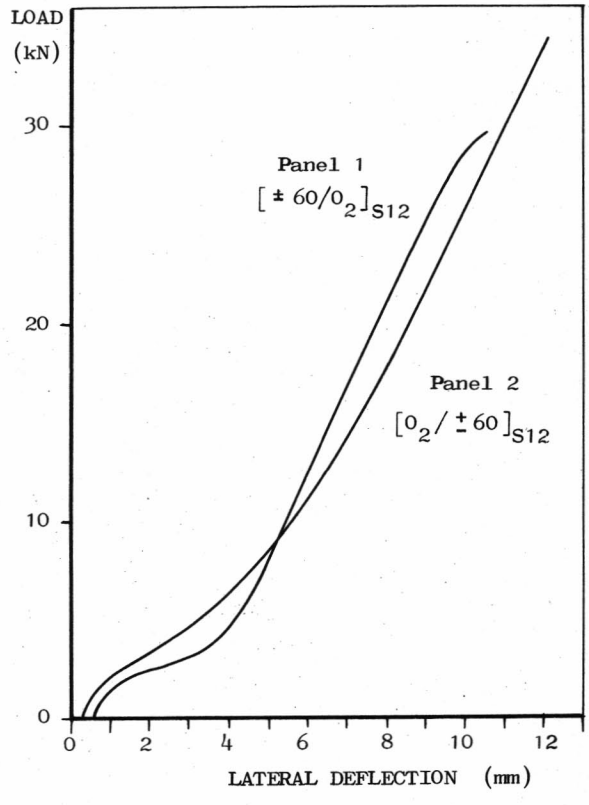

Figure 5. Lateral deflection of centre points of panels as function of load

Permanent deformation was observed as the panels were unloaded from approximately 15 kN and 20 kN for panel 1 and panel 2 respectively. At these load-levels crack-noises were picked up from the specimens indicating material damage in matrix.

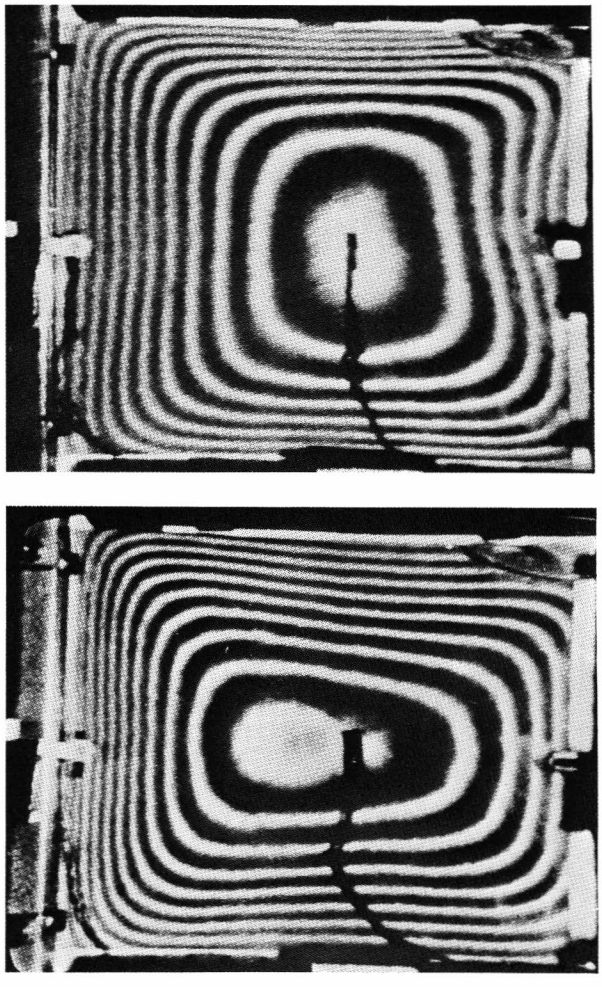

Figure 6. Moire' fringe pattern of the unstiffened panels, immediately prior to collapse. Top panel 1 (30 kN). Bottom panel 2 (35 kN)

Shear

The main results from the tests with the three plane panels are shown in Figs. 7, 8 and 9. In Fig. 7 the total shear deformations of the plane panels are plotted. Only panel 1 showed any permanent deformation. One can clearly see, from Fig. 7, how the stiffness of the panels increases with increasing percentage 90^{o}-layers. The results are not quite comparable since panels nos. 1 and 3 have 8 layers, whereas panel no. 2 has 10.

Fig. 8 shows the maximum lateral deflection evaluated from the Moire' patterns. Here the stiffening influence of the 90^{o}-layers is apparent. Fig. 9 shows an example of the buckling pattern as it appears by use of the shadow Moire' method. The picture is from the test with panel no. 3 and is taken immediately before failure at 125 kN. Because of the large deflections, the distance from the grid to the test specimen was too large at certain places and this makes the fringes somewhat blurred.

All three panels failed in a very similar way. Scattered matrix and fibre failures could be found on several places in the panels as well as delamination failures between the layers.

The tests with the three U-beams showed no significant change in buckling or collapse loads due to the change in flange stiffnesses.

The buckling and failure behaviour of the three U-beams was almost identical and the difference in buckling and collapse loads was less than 7 per cent. No permanent shear deformation could be measured. The first sounds of matrix failure was heard at a load of approximately $0.75 \cdot P_u$.

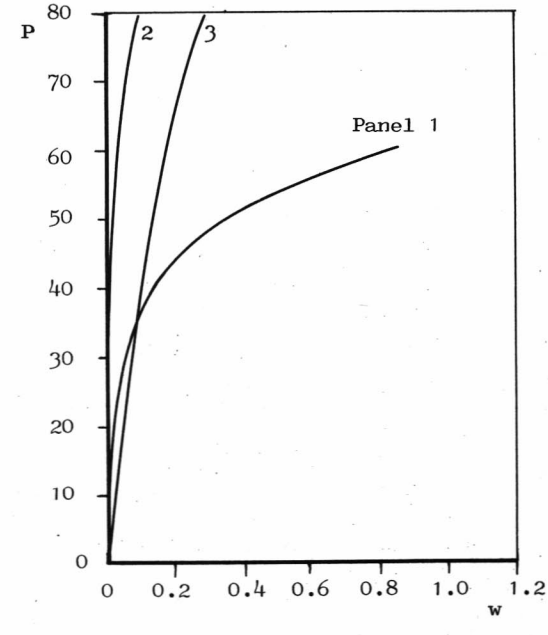

Figure 7. Total shear deformation curves. Plane shear panels nos. 1, 2 and 3

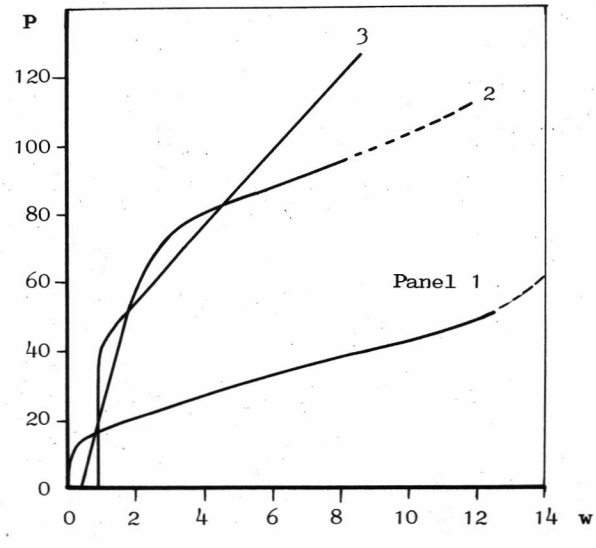

Figure 8. Lateral deflection curves evaluated from the Moire' patterns. Plane shear panels nos. 1, 2 and 3

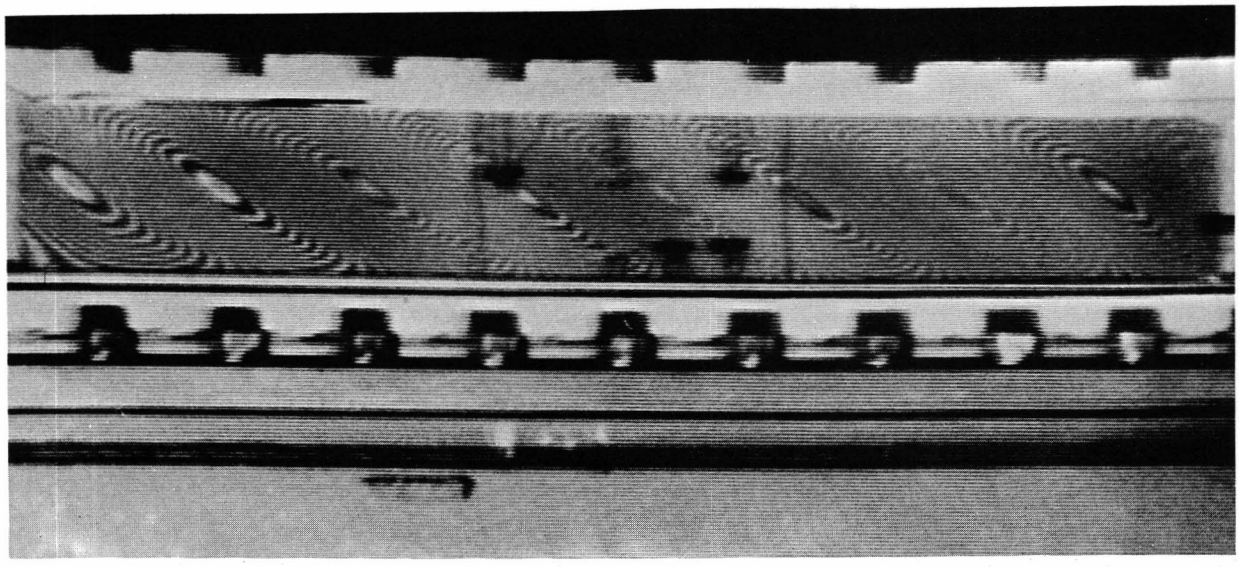

Figure 9. Moire' fringe pattern, plane shear panel no. 3

III. Theoretical Analysis

COMPUTER CODES AND METHODS OF CALCULATION

In the theoretical analyses of the tested specimens the STAGS C computer code was used for calculation of bucklings loads, deformation and stresses. The STAGS C code uses the finite difference procedure for finding the solution function to a set of partial differential equations which define the static equilibrium of a shell structure. Numerical values of the solution function are computed at a number of points on the shell surface.

Both linear bifurcation buckling analysis and nonlinear analysis was performed on the different types of structures that were tested, in order to evaluate buckling loads and buckling characteristics. In addition, minicomputer codes developed at the FFA were used to compute laminate stiffnesses and strengths from basic material properties and also for the compression loaded specimens, local buckling loads were computed by use of the Raleigh-Ritz method.

MODELS

The unstiffened compression loaded panels and all types of shear loaded panels were modelled into finite difference meshs as seen in Fig. 10. Node points, at which stresses and deformations were computed, were generated by a number of Rows and Columns. Edge conditions were chosen to satisfy the expected buckling modes.

The compression loaded stiffened panel was not analysed by use of the STAGS C code, but local buckling loads for the sections between and under the hat-stiffeners were computed by the Raleigh - Ritz procedure with simply supported edge conditions.

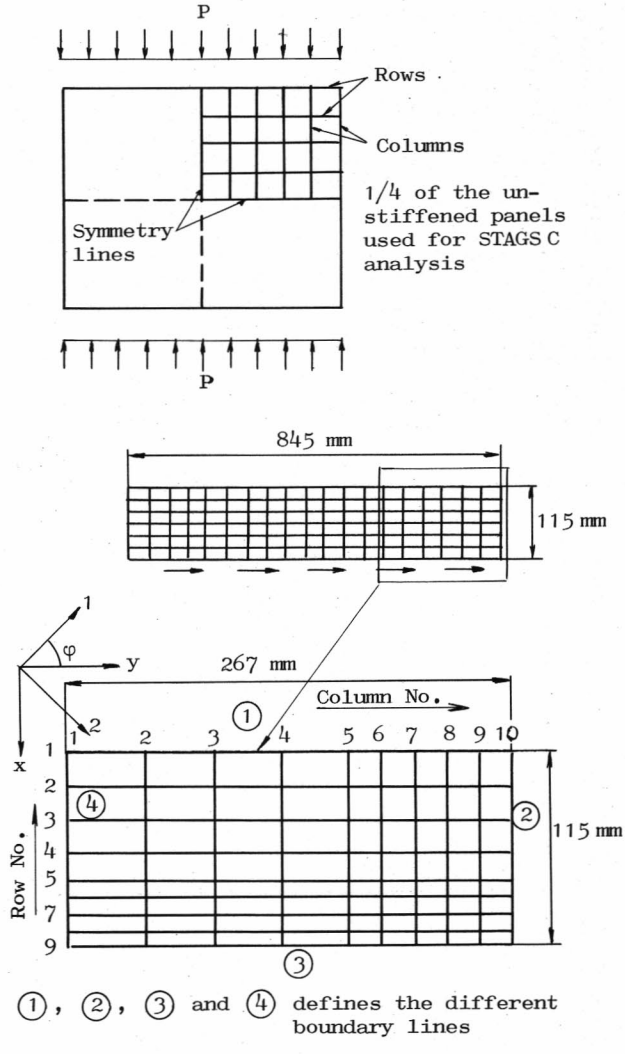

Figure 10. STAGS C models of the tested panels

The models used in the STAGS C analysis of the shear panels were of two kinds. At the bifurcation analysis a model of the whole panel was used to get a complete picture of the buckling mode. In order to reduce the computer costs, the non-linear analysis was carried out for a model covering about one third of the whole panel. The size of this model was determined from the results from the bifurcation analysis.

FAILURE CRITERIA

In the non-linear analysis of the unstiffened panels subjected to axial compression, the Tsai failure criterion was programmed into the STAGS C code.

$$\varphi = \sqrt{\left(\frac{\sigma_1}{\sigma_{1F}}\right)^2 + \left(\frac{\sigma_2}{\sigma_{2F}}\right)^2 - \frac{\sigma_1 \sigma_2}{\rho \sigma_{1F} \sigma_{2F}} + \left(\frac{\tau_{12}}{\tau_{12F}}\right)^2}$$

where $\rho = \frac{\sigma_{1F}}{\sigma_{2F}}$ and subscribed F denote the failure stresses.

The panels were expected to exceed the buckling loads by large and therefore it was necessary to study the stresses in the panel layers at high load levels. By listing only the 20 th largest Tsai-factors with corresponding stresses it was easy to evaluate in what layers and at what node points stresses might be critical, which also reduced the amount of output to a minimum.

The stresses calculated for the three plane shear panels, by use of the non-linear STAGS C analysis, were used to estimate the failure loads of the panels. This was made by use of the Tsai failure criterion and the results are presented in Fig. 11. The correlation between theoretical and experimental values was reasonably good.

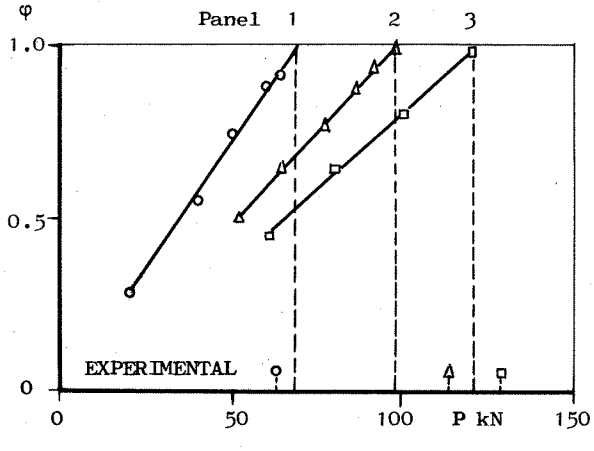

Figure 11. Failure loads of plane shear panels Nos. 1, 2 and 3 according to Tsai's failure criterion based on stresses calculated by use of the STAGS C computer program

IV. Comparison between experimental and theoretical results

The computed buckling loads for the unstiffened compression loaded panels coincided well with experimentally found values, but the computed collapse loads were approximately 100 % higher than the experimental. Fig. 12 shows the obtained results from the compression loaded panels. The stiffened panel was only theoretically analysed for local buckling and results from this panel can not be compared with the results from the unstiffened panels.

Specimens	Buckling loads (N)		
	fiber layered	experiment	theory
hat-stiffened panel	$(0_2/\pm 45)_{S8}$	~21 500 *)	22 680 *)
unstiffened panels	$[0_2/(\pm 60)_2]_{S12}$	~2 000	1 840
	$[(\pm 60)_2/0_2]_{S12}$	~2 000	2 200
Ultimate loads (N)			
hat-stiffened panel	$(0_2/\pm 45)_{S8}$	130 000	-
unstiffened panels	$[0_2/(\pm 60)_2]_{S12}$	~35 000	~70 000
	$[(\pm 60)_2/0_2]_{S12}$	~30 000	~65 000

*) local buckling of plate between stiffeners

Figure 12. Experimental and theoretical results of the compression loaded panels

There were several factors that affected the tested specimens which could not be considered in the theoretical models, such as material imperfections, the actual degree of freedom of motion valid at the supported panel ends and the rigidity of the test devices. Also due to the complex micro mechanical behaviour of fiberlayered materials, which could not be analysed in the STAGS C models, it was not expected that the ultimate loads could be accurately predicted for the compression loaded panels. However, the approximate location of the initial failure as estimated in the theoretical analysis coincided well with experimental observations.

The buckling modes of the six shear panels, calculated by bifurcation analysis, agreed very well with those of the experiments. This was also the case with the theoretical failure loads. The buckling loads, on the other hand, are more difficult to estimate with high

precision since the boundary conditions of the test specimens are hard to simulate in the theoretical analysis. The deflection curves of the plane panels, Fig. 13, show the strongly non-linear behaviour of the panels loaded in shear. The deflection curves from the experiments showed the same non-linear behaviour. See Fig. 8.

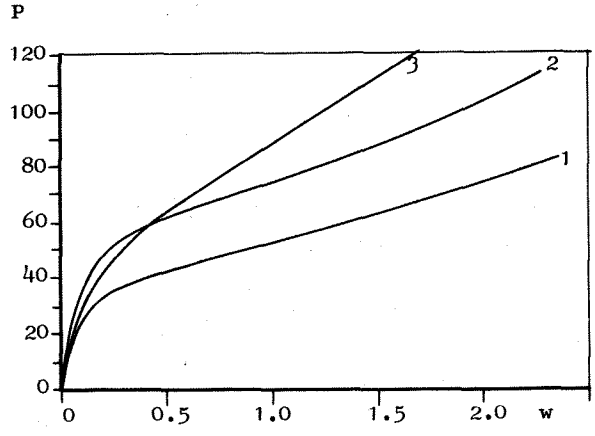

Figure 13. Theoretical lateral deflection curves from the non-linear STAGS C analysis. Plane shear panels 1, 2 and 3

V. Conclusions

The tests with all unstiffened panels indicated that the collapse load well exceeds the buckling loads in this kind of structures. Although a thorough investigation of the fracture behaviour of CFRP structures, under this type of loading, calls for a much more extensive investigation than the one related in this paper, it is evident that the highest permitted load very well may exceed the buckling load. As a whole, the CFRP panels appeared very 'ductile' and the ratio P_u/P_c was as high as 15 for the compression loaded panels and 3 for the shear loaded panels. Small permanent deformation was found in the compression tests but none in the shear tests.

The buckling load and buckling behaviour of the structures are very much dependent on the geometry and lay-up configuration, but the torsional stiffness of the flanges of the shear loaded U-beams had no significant influence on the buckling behaviour of the web.

As for the stiffened panel no global buckling occurred and the local-buckling load was very close to the collapse load.

The theoretical analysis carried out by use of the STAGS C computer code showed that the type of buckling (buckling mode) can be estimated with high precision using the bifurcation analysis. The buckling load, on the other hand, is preferably calculated by use of a non-linear analysis. Using this method, the buckling load can be estimated within reasonable tolerances, but the result is very much dependent on the model used and to what extent the actual boundary conditions and imperfections of the test specimens are resembled in the theoretical analysis. This requires a considerable amount of experience of the program user. This is also the case with the calculation of the failure load. If the model, boundary conditions etc. are in good agreement with the structure considered, the failure load can be estimated, using for instance the Tsai-failure criterion, with acceptable accuracy.